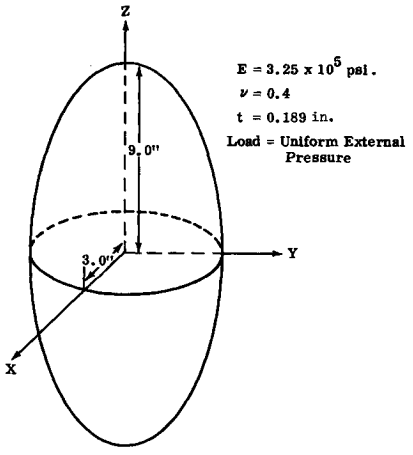

Fig. 2 Axisymmetrically pressurized prolate spheroid.

Numerical Examples

The use of the method is demonstrated by its application to two shell buckling problems presented below. The first problem involves a large, ring-stringer eccentrically reinforced cylinder (Fig. 1).‡ The loading was a fixed internal stabilizing pressure of 31 psi, in combination with a variable compressive end load. Classical simple support boundary conditions were utilized to enable comparison with Refs. 6 and 7. The idealization used consisted of 20 segments for the whole structure. Comparisons of the analytical results are presented in Table 1. The over-all critical mode was found to be $n = 0$, $m = 13$, where n is the number of circumferential waves and m the number of longitudinal half-waves. Table 1 shows the analytical results for the $n = 0$ calculations, and it can be seen again that the convergence characteristics are excellent. By the fourth pass, the change from anticipated to corrected value of the critical load is only 0.00017%, moreover, the estimates of some of the higher eigenvalues show an average difference of 0.57% (with a maximum of 2.0%) for the first 11 roots, and an average difference of 2.72% (with a maximum of 10%) for the first 18 roots, when compared to Ref. 7. Thus, when the first root is converged, excellent estimates are available for a large number of the higher roots. The results from Refs. 6, 7 and the current work should be close, but do not have to agree exactly, due to differences in shell theories and formulations. No difficulty was encountered in obtaining eigenvalues corresponding to eigenvectors with many waves in a segment or with load reversals.

The second problem considered is a prolate spheroidal shell under a uniform external pressure as shown in Fig. 2. The results obtained with the present approach are compared to experimental and other theoretical results in Table 2. It can be seen that the results from the three numerical integration techniques are all very close to the experimental predictions.

Table 2 Comparison of results for prolate spheroid

Harmonic shape	Buckling load, psi		
	$n = 2$	$n = 3$	$n = 4$
Current method	208.3	138.39	174.1
Experimental (Ref. 8)	—	137.0	—
Theoretical (Ref. 8)	> 197.0	> 197.0	197.0
Ref. 3	208.8	138.7	174.0
Ref. 4	—	139.23	—

‡ Notes on Fig. 1: Loading—compressive end load is N, internal stabilization pressure is 31 psi; Boundary conditions—ends are simply supported.

References

[1] Svalbonas, V. and Balderes, T., "A Procedure for Extending the STARS II Digital Computer Program to Shell Buckling Analysis," Grumman ADN 02-01-71.1, May 1971.

[2] Svalbonas, V., "Numerical Analysis of Shells—Vol. I: Unsymmetric Analysis of Orthotropic, Reinforced Shells of Revolution," CR-61299, Sept. 1969, NASA.

[3] Cohen, G., "Computer Analysis of Asymmetric Buckling of Ring Stiffened Orthotropic Shells of Revolution," AIAA Paper 67-109, New York, Jan. 1967.

[4] Kalnins, A., "Static, Free Vibration, and Stability Analysis of Thin, Elastic Shells of Revolution," AFFDL-TR-68-144, March 1969, Wright-Patterson Air Force Base, Ohio.

[5] Hurty, W. and Rubinstein, M., *Dynamics of Structures*, Prentice-Hall, Englewood Cliffs, N.J., 1965.

[6] Dickson, J. and Brolliar, R., "The General Instability of Eccentrically Stiffened Cylindrical Shells under Axial Compression and Lateral Pressure," CR-1280, Jan. 1969, NASA.

[7] Block, D., Card, M., and Mikulas, M., "Buckling of Eccentrically Stiffened Orthotropic Cylinders," TN D-2960, Aug. 1965, NASA.

[8] Hyman, B. and Healey, J., "Buckling of Prolate Spheroidal Shells under Hydrostatic Pressure," *AIAA Journal*, Vol. 5, No. 8, Aug. 1967, pp. 1469–1477.

Effect on Supersonic Jet Noise of Nozzle Plenum Pressure Fluctuations

RAYMOND KUSHIDA* AND JACK RUPE†
Jet Propulsion Laboratory, Pasadena, Calif.

THE proportion of the total engine noise which is attributable to the jet plume in a jet propulsion device increases markedly as the exhaust velocity increases.[1] When the jet velocity is nearly sonic or supersonic, then the jet noise can overwhelm other noise sources. In this preliminary study it is found that the interaction of upstream disturbance with a supersonic jet plume causes an increase in the total noise. It is expected that this added insight into jet noise sources will be useful in devising improved methods of noise reduction in future jet engines.

The noise radiated from a supersonic jet plume was measured and the sound power was correlated with the pressure fluctuations measured in the chamber. A research liquid rocket engine using the propellant combination hydrazine and nitrogen tetroxide was used to generate a wide range of chamber pressure fluctuation. Previous experience at JPL with that propellant combination had shown that very smooth combustion could be

Table 1 Rocket engine geometric characteristics

Length (injector to throat)	1.17 m (46 in.)
Chamber diameter	0.28 m (11 in.)
Nozzle throat diameter	0.197 m (7.76 in.)
Throat wall cuvature radius	0.199 m (7.84 in.)
Nozzle exit diameter	0.228 m (8.95 in.)
Nozzle divergence half angle	15°

Received December 30, 1971; revision received March 14, 197
This paper represents the results of one phase of research carried out a the Jet Propulsion Laboratory, California Institute of Technolog under Contract NAS7-100 sponsored by NASA.

Index categories: Aircraft Propulsion System Noise; Liquid Rock Engines; Jets, Wakes, and Viscid-Inviscid Flow Interactions.

* Member of the Technical Staff, Liquid Propulsion Combustio Research Group.

† Supervisor, Liquid Propulsion Combustion Research Group.

Table 2 Rocket engine operating characteristics

Run number	B1332	B1322
Injector configuration	46 like doublets	47 unlike doublets
N_2O_4/N_2H_4 mass flow ratio	1.265	1.170
Chamber stagnation pressure	1.43 MN/m^2 (207 psia)	1.42 MN/m^2 (206 psia)
Characteristics velocity (c^*)	1672 m/s (5485 fps)	1729 m/s (5664 fps)
Combustor efficiency (η_{c*})	94.47%	97.14%
Chamber pressure fluctuations, rms	7 kN/m^2	80 kN/m^2
OAPWL db re 10^{-13} w	181.9	190.6
Nozzle exit velocity	1264 m/s	1270 m/s
Jet velocity[a]	2405 m/s	2410 m/s
Jet velocity/atmos. sound speed	7.1	7.1

[a] Isentropic expansion to 93 kN/m^2 (13.5 psia).

achieved with injector elements which impinge fuel on fuel and oxidizer on oxidizer (like impinging doublets) and very rough combustion was obtained if there was direct impingement of liquid fuel on liquid oxidizer (unlike impinging doublets).[2,3] The engine is the one designated as RMIR No. 7 in Ref. 2. Its geometric characteristics are listed in Table 1. The injector face has baffles 16 cm (6 in.) long to prevent the tangential and radial modes of instability. The chamber had water cooled Photocon pressure transducers mounted on the injector face and at a station 97 cm (38 in.) from the injector.

The engine was mounted horizontally with the jet center line approximately 1 m (3 ft) off the hard pan ground surface. A set of 8 to 10 Bruel and Kjar $\frac{1}{4}$ in. microphones were directed at the jet centerline from a position 1 m above the ground on stakes located 10 m from the jet axis. Thrust and propellant flows were measured. Operating conditions are listed in Table 2 for a typical smooth and a typical rough run.

The output from the pressure transducers and the microphones were recorded simultaneously on magnetic tape recorders using AC coupled amplifiers. The microphones were calibrated daily using a Pistonphone. The Photocon transducer response is modified by diaphragm resonance at frequencies above 10 kHz; hence an rms meter incorporating sharp cutoff filters for frequencies below 100 Hz and above 8500 Hz was utilized to give a constant bandwidth to the monitored signal. The same rms meter was used to process the microphone data. Later comparison with a wider band rms meter showed the cutoff frequencies may have decreased the sound pressure level values by about 1.5 db. Since the same factor will apply to all noise measurements reported herein, this source of error was neglected in this preliminary test. The nozzle plenum chamber pressure fluctuations were measured by a roughness intensity, $(\Delta p_{rms}/P_{tot}) * 100$. The mean total pressure in the nozzle plenum, P_{tot}, was computed using time average static pressure, the contraction ratio and the equilibrium expansion properties of the combustion products.

To obtain the over-all sound power, the sound intensity values were integrated over the spherical surface enclosing the jet nozzle. A mean curve of sound intensity versus direction taken from Potter[4] was used to extrapolate measurements to the jet axis. The resulting sound power, W_A, was expressed in watts and can be normalized using the jet mechanical power, W_J, to form the acoustic efficiency. The mechanical power was computed from

$$W_J = \tfrac{1}{2}(\text{thrust})^2/(\text{mass flow rate}), \text{ watts}$$

and the acoustic efficiency in percentage was then

$$\eta_A = 100\, W_A/W_J$$

The results are presented in Fig. 1,‡ where acoustic efficiency is plotted as a function of nozzle plenum pressure fluctuation.

The pressure fluctuations measured in the combustion chamber ranged from 6 rms kN/m^2 (0.8 rms psi) to an extreme of 410 rms kN/m^2 (61 rms psi). Examination of the frequency spectrum and of the oscillograph playbacks of the rough runs indicated that these runs exhibited resonant combustion. This was particularly true in the single extremely rough run where peak to peak pressure amplitudes reached 2500 kN/m^2 (370 psi), imposed on a mean chamber pressure of 1400 kN/m^2 (200 psi). The fundamental mode of oscillation was the longitudinal mode at about 580 Hz although there were noticeable peaks in the higher modes of the classic cylindrical cavity oscillation. The spectral analysis of noise detected at the microphones showed a small peak at the fundamental frequency, but the power involved in the peak was rather small.

The mixture ratio ranged from O/F of 0.91 to 1.67 and the chamber pressure from 1160 kN/m^2 (169 psi) to 1420 kN/m^2 (206 psia). No trend with either mixture ratio or chamber pressure was apparent in the noise data.

For the smooth runs, the measured acoustic efficiency which ranges from 0.27 to 0.34% are in reasonable accord with a correlation presented by Guest[5] in which an engine of this size range should have an efficiency of about 0.29%. The correlating line drawn in Fig. 1 is not extended below 0.3% since this seems a reasonable lower limit for jet noise in smooth running practical engines.

In this study it has been shown that pressure fluctuations in the plenum chamber to a supersonic nozzle can strongly increase the noise radiated from the jet plume. The correlation in Fig. 1 shows that jet noise acoustic efficiency increases from 0.3% to 0.8% (or 4 db) when the chamber roughness intensity increases from essentially no plenum chamber roughness to 2%. A roughness level of 2% has been observed in some turbojet engines.[6] It is concluded that the reduction or elimination of plenum chamber pressure fluctuations may be an important method of reducing the total noise from jet engines.

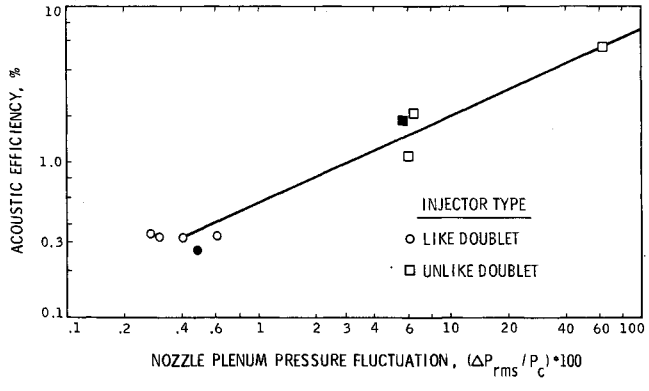

Fig. 1 Experimental correlation of jet noise acoustic efficiency with nozzle plenum chamber pressure fluctuation.

References

[1] Lighthill, M. J., "Jet Noise," *AIAA Journal*, Vol. 1, No. 7, July 1963, pp. 1507–1517.

[2] Rupe, J. H. et al., "An Experimental Correlation of the Nonreactive Properties of Injection Schemes and Combustion Effects in a Liquid Propellant Rocket Engine," TR 32-255, Sept. 1967, Parts I, II, V, Jet Propulsion Laboratory, Pasadena, Calif.

‡ In Fig. 1 the round solid symbol is run B1332 and the square solid symbol indicates run B1322 which are the typical smooth and the typical rough run, respectively, given in Table 2.

[3] Clayton, R. M., "Experimental Observations Relating the Inception of Liquid Rocket Engine Popping and Resonant Combustion to the Stagnation Dynamics of Injection Impingement," TR 32-1479, Dec. 1970, Jet Propulsion Laboratory, Pasadena, Calif.

[4] Potter, R. C. and Crocker, M. J., "Acoustic Prediction Methods for Rocket Engines," CR-566, Oct. 1966.

[5] Guest, S. H., "Acoustic Efficiency Trends for High Thrust Boosters," TN-D-1999, July 1964, NASA.

[6] Bonnell, J. M., Marshall, R. L., and Riecke, G. T., "Combustion Instability in Turbojet and Turbofan Augmentors," AIAA Paper 71-698, Salt Lake City, Utah, June 1971.

Accuracy of Third-Order Predictor-Corrector Difference Schemes for Hyperbolic Systems

P. WESSELING*

National Aerospace Laboratory, Amsterdam, Netherlands

THIS Note deals with numerical methods for the following system of equations:

$$\partial\phi/\partial t+\partial f(\phi,x,t)/\partial x=0 \tag{1}$$

where $\phi^T=(\phi_1,\phi_2,\ldots,\phi_n)$, $f^T=(f_1,f_2,\ldots,f_n)$. The system is assumed to be hyperbolic. Equation (1) is of great importance in fluid mechanics, because both the equations of inviscid gas dynamics and the advection operator are of this form.

Difference schemes for the numerical solution of Eq. (1) should preferably be of predictor-corrector type, because then the matrix $F=\partial f/\partial\phi$ and its derivatives do not appear in the difference scheme. This eliminates time-consuming matrix multiplications. An often-used predictor-corrector scheme for the solution of Eq. (1) is the Lax-Wendroff scheme, as formulated by Richtmyer.[1] A third-order predictor-corrector scheme has been constructed by Rusanov[2] and by Burstein and Mirin.[3] This difference scheme derives special significance from the fact that it can be shown,[4] that there exists no other third-order predictor-corrector scheme for Eq. (1).

The Rusanov-Burstein-Mirin (RBM) scheme contains two parameters which may vary. One is the fraction $\tau\Delta t$ of the time-step Δt at which the first predictor is evaluated. The other is the damping coefficient ω. The parameter τ does not influence the amplification matrix (for a definition see Ref. 1), and therefore has only little influence on the accuracy. We will take $\tau=\frac{1}{3}$. The parameter ω has a large influence on the accuracy, as will be demonstrated. Furthermore, it will be shown that it is possible to improve the accuracy of the RBM scheme considerably by modifying the damping term.

The RBM scheme is defined as follows:

$$\phi^{(1)}_{j+1/2}=\tfrac{1}{2}(\phi^n_{j+1}+\phi^n_j)-(\sigma/3)(f^n_{j+1}-f^n_j) \tag{2}$$

$$\phi^{(2)}_j=\phi^n_j-\tfrac{2}{3}\sigma(f^{(1)}_{j+1/2}-f^{(1)}_{j-1/2}) \tag{3}$$

$$\phi^{n+1}_j=\phi^n_j-(\sigma/24)(-2f^n_{j+2}+7f^n_{j+1}-7f^n_{j-1}+2f^n_{j-2})-\tfrac{3}{8}\sigma(f^{(2)}_{j+1}-f^{(2)}_{j-1})+D \tag{4}$$

$$D=-\tfrac{1}{24}\omega\delta^4\phi^n_j \tag{5}$$

where $\sigma=\Delta t/\Delta x$ and $\delta^4\phi^n_j$ is an undivided fourth difference. Equations (2)–(4) are called the first predictor, the second predictor, and the corrector, respectively. The quantity D is called the damping term. For stability it is necessary that the damping-coefficient ω satisfy

$$c_m^2(4-c_m^2)\leqq\omega\leqq 3 \tag{6}$$

where the Courant number c_m is defined as $c_m=\sigma|\lambda_m|$, with λ_m the absolutely largest eigenvalue of F in the point $(n\Delta t, j\Delta x)$.

In order to exhibit the influence of ω on the accuracy, a model problem with one unknown is studied, with $f=u\phi$ $u=(a+b\cos^2\pi x)^{-1}$. For the determination of the errors in th numerical calculations use is made of the fact that with $\phi(0,x$ periodic in x with period 1 the exact solution is periodic in with period $a+b/2$.

Received January 4, 1972.

* Senior Research Engineer.

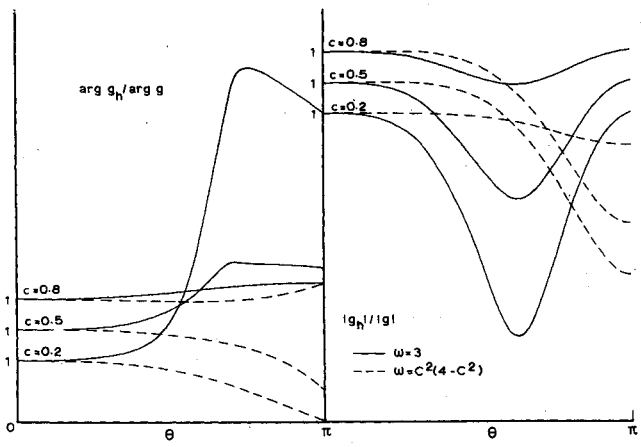

Fig. 1 Dispersion and dissipation of the Rusanov-Burstein-Mirin scheme.

The following four cases were calculated: case 1: $a=b=1$ $\phi(0,x)=H(x-\frac{1}{2})$; case 2: $a=b=1$, $\phi(0,x)=\sin^2\pi x$; case 3 $a=1.05$, $b=1.9$, $\phi(0,x)=H(x-\frac{1}{2})$; case 4: $a=1.05$, $b=1.9$ $\phi(0,x)=\sin^2\pi x$; where $H(x)$ is the periodic step function wit period 1: $H(x)=0$ for $2m-1<x\leqq 2m$, $H(x)=1$ for $2m<x\leqq 2m+1$, with m an arbitrary integer. Table 1 gives for tw values of ω the average error ε, defined as

$$\varepsilon=\Delta x\sum_{j=0}^{j=1/\Delta x}|\phi^n_j-\phi(n\Delta t,j\Delta x)| \tag{7}$$

where ϕ is the exact (analytical) solution.

Table 1 shows that the accuracy depends strongly on th damping coefficient ω, especially when the solution is smoot This can be explained by a study of the difference between th amplification matrix of the differential equation and the ampl fication matrix of the difference scheme. With only one unknow these matrices reduce to factors g and g_h, respectively. Th amplification factor is the factor by which a harmonic wa $\exp(i\theta x/\Delta x)$ is multiplied when it is propagated over a tim interval Δt by the differential equation or the difference schem Figure 1 represents the quantities $|g_h/g|$ and $\arg g_h/\arg g$ functions of θ, for several values of the Courant number $c=\sigma$ These quantities will be called the dissipation and dispersio respectively. The figure shows that the amplification factor g_h strongly influenced by the damping coefficient ω, so that it is n surprising that ω has a large influence on the accuracy of t RBM scheme. Long waves, with little dispersion, are damp more strongly with $\omega=3$ than with $\omega=c^2(4-c^2)$. On the oth hand, short waves which have much dispersion for both values ω are damped strongly with $\omega=c^2(4-c^2)$, but weakly or not all with $\omega=3$. Clearly, with $\omega=c^2(4-c^2)$ the RBM sche has much better dissipation and dispersion properties than w $\omega=3$.

The question arises of whether there exists a better choice ω than $\omega=c^2(4-c^2)$. This is probably not the case, beca the value $c^2(4-c^2)$ is singled out by the fact, that with u constant the RBM scheme is fourth order accurate in x rat than third order.

When the number of unknowns is greater than one assumption of hyperbolicity implies the existence of a matri with the property $UFU^{-1}=\Lambda$, with Λ a diagonal matrix. I the study of dissipation and dispersion F is assumed to constant. The diagonalized system then consists of n mutu independent equations, each with one unknown. The differe scheme for the kth unknown has the following damping term

$$D=-\tfrac{1}{24}\omega\delta^4\psi^n_{k,j}$$